

Sensitivity of Curie Temperature to Crystal-Field Anisotropy. II. FeF₂

M. E. LINES

*Bell Telephone Laboratories, Murray Hill, New Jersey**

(Received 28 November 1966)

FeF₂ is a simple two-sublattice antiferromagnet and has a rutile crystal structure. Its large anisotropy can be represented to a good approximation by single-ion crystal-field terms of the type discussed in Paper I. The purpose of the present paper is, firstly, to analyze relevant high- and low-temperature experimental data in order to estimate as accurately as possible the important exchange and anisotropy parameters for FeF₂ and, secondly, to use this information to test the various theories for transition temperature which were the subject of Paper I. An adequate spin Hamiltonian for FeF₂ can be written as

$$\mathcal{H} = \sum_{nn} J_1 \mathbf{S}_i \cdot \mathbf{S}_j + \sum_{nnn} J_2 \mathbf{S}_i \cdot \mathbf{S}_j - \sum_i D S_{iz}^2,$$

where \sum_{nn} (\sum_{nnn}) is over all pairs of nearest (next-nearest) neighbor spins S_i and S_j , and where \sum_i is over all spins in the system. From an analysis of nuclear-resonance and magnetic-susceptibility data we find $D = 6.5 \pm 0.3$ cm⁻¹, $J_2 = 3.85 \pm 0.2$ cm⁻¹, and $J_1/J_2 = 0.1 \pm 0.25$. The resulting ratio $D/J_2 = 1.7 \pm 0.2$ takes FeF₂ outside the small anisotropy range for which the theory of Paper I was primarily developed. Even so, use of the above parameter values in that theory results in a theoretical estimate for the Néel temperature which is in error by only some 12% for FeF₂. This estimate is considerably more accurate than those obtained by use of molecular-field theory or by earlier Green's-function approximations.

1. INTRODUCTION

FERROUS fluoride is a simple two-sublattice antiferromagnet and has the rutile crystal structure with Fe²⁺ cations on a body-centered tetragonal lattice. It is of interest in the present context primarily because the spin Hamiltonian derived from crystal-field theory, which can be used to discuss the magnetic properties of this salt, contains sizeable single-ion crystal-field anisotropy terms of the type discussed in Paper I. The object of the present paper is to estimate as accurately as possible the exchange and anisotropy parameters of the system (by discussing the high- and low-temperature magnetic properties for which reasonably accurate and well-tried theoretical procedures are available), and to use these results to check the as yet completely untested theories for transition temperature which were the subject of Paper I. Such a check is particularly important in view of the widely differing results obtained from the theories as yet put forward to discuss the effects of crystal-field anisotropy on transition temperatures.

FeF₂ is also of interest since, together with MnF₂ and CoF₂, it forms a series of isomorphous crystals which all exhibit a simple two-sublattice antiferromagnetism at low temperatures with spins aligned along the tetragonal c_0 axis. Earlier papers¹⁻³ on MnF₂ and CoF₂ have indicated that for both these salts the nearest-neighbor exchange J_1 (between neighboring spins along the c_0 axis) is an order of magnitude smaller than the exchange J_2 between next-nearest neighbors. The present investigation indicates that this surprising feature is common to the ferrous salt as well. This distinctive property could make the series Mn²⁺(3d⁵), Fe²⁺(3d⁶),

and Co²⁺(3d⁷) in the rutile-structured difluorides a profitable source of study for theorists interested in superexchange mechanisms.

Crystal-field theory for Fe²⁺ in an environment with rutile crystal symmetry has been adequately discussed by Tinkham⁴ and by Honma.⁵ The free-ion ground state is ⁵D and the orbital degeneracy is completely lifted by the rhombic crystal field. Spin-orbit effects are adequately treated by perturbation methods, the effective Hamiltonian pertaining to the lowest orbital state of a single ferrous ion being

$$\mathcal{H} = -D S_z^2 + E(S_x^2 - S_y^2), \quad (1.1)$$

where z is the c_0 axis (see Fig. 1) and where the coefficients D and E contain significant contributions from spin-spin interactions within the Fe²⁺ ion (Pryce⁶) and are therefore not simply related to the spin-orbit coupling constant λ . The spin quantum number is $S = 2$, and small (and almost certainly negligible⁴) quartic terms have been omitted from (1.1).

Combining paramagnetic resonance and magnetic susceptibility experimental results obtained for Fe²⁺ in ZnF₂, Tinkham⁴ was able to show that $E \sim 0.1D$ for that case. A similar result is almost certain to hold for FeF₂ itself because of the isomorphism of ZnF₂ and FeF₂ coupled with their almost identical unit-cell dimensions. In Sec. 2 we show that the rhombic anisotropy E contributes to bulk magnetic properties as $(E/D)^2$ and may therefore be safely neglected. It follows that a suitable spin Hamiltonian for the entire lattice of Fe²⁺ ions can be written in the form

$$\mathcal{H} = \sum_{\langle i,j \rangle} J_{ij} \mathbf{S}_i \cdot \mathbf{S}_j - \sum_i D S_{iz}^2, \quad (1.2)$$

where J_{ij} is the exchange interaction between spins S_i

* Work performed at Clarendon Laboratory, Oxford University, Oxford, England.

¹ G. G. Low, Proc. Phys. Soc. (London) **82**, 992 (1963).

² G. G. Low, A. Okazaki, R. W. H. Stevenson, and K. C. Turberfield, J. Appl. Phys. **35**, 998 (1964).

³ M. E. Lines, Phys. Rev. **137**, A982 (1965).

⁴ M. Tinkham, Proc. Roy. Soc. (London) **A236**, 535 (1956).

⁵ A. Honma, J. Phys. Soc. Japan **15**, 456 (1960).

⁶ M. H. L. Pryce, Phys. Rev. **80**, 1107 (1950).

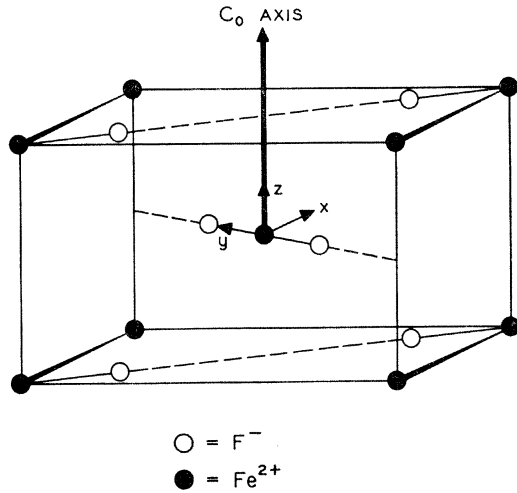


FIG. 1. The rutile crystal structure with axes x, y, z , as used in the text.

and S_j and is summed over all pairs ij in the lattice. Strictly speaking, we should allow for exchange anisotropy⁷ and for dipole-dipole anisotropy in addition to the crystal-field term. For FeF_2 , both these terms are very small compared with the crystal-field anisotropy and their effects can, to a fair approximation, be assumed to be contained in the parameter D although, more exactly, they have a more complicated spin dependence than that indicated in (1.2). The dipole-dipole contribution is not difficult to estimate and proves to be $\sim 5\%$ of D ; the exchange anisotropy contribution we have not assessed and it will remain buried in the parameter D . However, order of magnitude estimates suggest that it is likely to be even smaller than the dipolar contribution.

In Sec. 2 we develop a spin-wave theory for FeF_2 and use it to interpret antiferromagnetic resonance and sublattice magnetization measurements obtained in the low-temperature region. The results are analyzed using Hamiltonian (1.2) assuming all exchange interactions more remote than next-nearest neighbor to be negligible (an assumption based on the study of possible superexchange paths, coupled with the findings² for MnF_2).

In Sec. 3 we calculate magnetic susceptibility and interpret the recent single-crystal susceptibility results of Foner.⁸ Both for $T \ll T_N$ and for $T \gg T_N$ ($T_N =$ Néel temperature) the susceptibility results may be interpreted reliably³ by molecular-field theory. Coupling our findings for Sec. 3 with those for Sec. 2, we are able to estimate $J_2 = (5.55 \pm 0.30)^\circ K$, $J_1/J_2 = 0.1 \pm 0.25$, and $D = 6.5 \pm 0.3 \text{ cm}^{-1}$, from which we calculate $D/J_2 = 1.7 \pm 0.2$.

This value for D/J_2 takes FeF_2 well outside the small anisotropy range for which the Green's-function theory of Paper I was developed. Nevertheless, in Sec. 4 we adapt the theory of Paper I for the present case and,

⁷ J. Kanamori, in *Magnetism*, edited by G. T. Rado and H. Suhl (Academic Press Inc., New York, 1963), Vol. 1.

⁸ S. Foner, in *Proceedings of the International Conference on Magnetism, Nottingham, 1964* (The Institute of Physics and The Physical Society, London, 1965), p. 438.

TABLE I. Comparison of predictions of various theories for the Néel point T_N of FeF_2 with $T_N(\text{expt.}) = 79^\circ K$.

Theory	$T_N(\text{theory})$ ($^\circ K$)	$T_N(\text{theory})/$ $T_N(\text{expt.})$
Molecular field	98.5	1.25
Green's function		
(i) Narath ^a decoupling	116	1.47
(ii) Anderson-Callen ^b decoupling	94	1.19
(iii) Paper I decoupling	88.5	1.12

^a See Ref. 10.

^b See Ref. 9.

using the values determined for exchange and anisotropy, compare the theoretical estimate for T_N with the observed Néel temperature for FeF_2 . The theoretical value is too high by some 12% (see Table I) but compares well with the estimates from molecular-field theory (+25%) and with those of the Green's-function theories of Anderson and Callen⁹ (+19%) and Narath¹⁰ (+47%). Since all of the Green's-function theories are expected to break down for highly anisotropic systems, predicting transition temperatures which are too high (see Paper I), overestimates for the present case are not surprising. It is possible to make some qualitative allowance for the high anisotropy breakdown of the Green's-function theories, and the final indications are that the theory of Paper I accounts fairly quantitatively for the sensitivity of T_N to crystal-field anisotropy in the intermediate anisotropy region ($D/J_2 \sim 1$), although it may still overestimate the effect by a few percent.

2. SPIN-WAVE THEORY

In this section we shall retain a rhombic crystal-field term in the spin Hamiltonian and show that it contributes to bulk magnetic properties only as (E/D) .² Thus, if $E/D \sim 0.1$, this result enables us to establish the fact that a spin Hamiltonian of the form (1.2) is sufficient for subsequent use, the rhombic terms affecting bulk properties by only $\sim 1\%$. This result is really evident from symmetry considerations alone, but we shall report the detailed calculations in order to point out some common errors which are frequently found in spin-wave analyses of crystal-field terms.

The basic rutile crystal structure is shown in Fig. 1. Noting that the corner cations and the body-center cations have environments which differ by a 90° rotation about the c axis, we write a Hamiltonian for the complete spin system in the form

$$\begin{aligned}
 \mathcal{H} = & \sum_u [E(S_{ux}^2 - S_{uy}^2) - DS_{uz}^2] \\
 & + \sum_d [E(S_{dy}^2 - S_{dx}^2) - DS_{dz}^2] \\
 & + \sum_{nn} J_1(\mathbf{S}_u \cdot \mathbf{S}_{u'} + \mathbf{S}_d \cdot \mathbf{S}_{d'}) + \sum_{nnn} J_2 \mathbf{S}_u \cdot \mathbf{S}_d. \quad (2.1)
 \end{aligned}$$

⁹ F. B. Anderson and H. B. Callen, *Phys. Rev.* **136**, A1068 (1964).

¹⁰ A. Narath, *Phys. Rev.* **140**, A854 (1965).

Here we have separated the system into its two sublattices, the "up" sublattice (u) and the "down" sublattice (d), noting that nearest-neighbor spins (J_1) are always on the same sublattice, and next-nearest neighbor spins (J_2) on different ones.

Since $E \ll D$, the ground state of the system will have an average spin per site which is close to saturation (contrast this³ with the case for CoF₂ for which $E > D$) and may be adequately described in terms of spin deviations from the Néel state. We therefore introduce Holstein-Primakoff spin variables for the "up" and the "down" sublattices¹¹ as follows

$$\begin{aligned} S_{uz} &= S - a_u^\dagger a_u, & S_u^+ &= (2S)^{1/2} a_u, \\ S_u^- &= (2S)^{1/2} a_u^\dagger; \end{aligned} \quad (2.2)$$

$$\begin{aligned} S_{dz} &= -S + b_d^\dagger b_d, & S_d^+ &= (2S)^{1/2} b_d^\dagger, \\ S_d^- &= (2S)^{1/2} b_d; \end{aligned} \quad (2.3)$$

where the boson operators $a, a^\dagger, b, b^\dagger$ satisfy the commutation relations

$$[a_u, a_{u'}^\dagger] = \delta_{uu'}, \quad [b_d, b_{d'}^\dagger] = \delta_{dd'}, \quad (2.4)$$

with all other commutators zero.

Equations (2.2) and (2.3) may now be used to express (2.1) in terms of the boson operators. Some words of caution are necessary at this juncture, however, concerning the representation of the anisotropy terms. Firstly, we consider the DS_z^2 axial anisotropy terms. For the "up" sublattice we find

$$S_{uz}^2 = S^2 - 2S a_u^\dagger a_u + a_u^\dagger a_u a_u^\dagger a_u, \quad (2.5)$$

and a common feature of many earlier spin-wave approximations is the assumption that the term $a_u^\dagger a_u a_u^\dagger a_u$ is negligible in the noninteracting spin-wave representation. This is not so; we should write

$$S_{uz}^2 = S^2 - (2S-1) a_u^\dagger a_u + a_u^\dagger a_u^\dagger a_u a_u, \quad (2.6)$$

where it is the final term on the right-hand side which is truly a spin-wave interaction or higher-order term, and which can be omitted in the noninteracting spin-wave approximation (which we shall use throughout this section). The neglect of $a_u^\dagger a_u a_u^\dagger a_u$ from (2.5) leads to spurious anisotropy effects which are particularly noticeable for $S = \frac{1}{2}$ for which case crystal-field terms give rise to no anisotropy (since $S_x^2 = S_y^2 = S_z^2 = \frac{1}{4}$).

Now let us consider the rhombic anisotropy $E(S_x^2 - S_y^2)$. Direct substitution from (2.2) leads to

$$\begin{aligned} S_{ux}^2 - S_{uy}^2 &= \frac{1}{2}(S_u^+ S_u^+ + S_u^- S_u^-) \\ &= S(a_u a_u + a_u^\dagger a_u^\dagger). \end{aligned} \quad (2.7)$$

But neither is this a correct representation in terms of the boson operators. For a satisfactory simple spin-wave theory, we require that the spin operators should be related to boson operators in such a way that all the single-spin operators contained in the Hamiltonian have the correct matrix elements at least between and within

the ground- and first excited single-spin states. Consider, for example, the operator S_{uz}^2 . In single-spin states $|S\rangle$ and $|S-1\rangle$ it has eigenvalues S^2 and $(S-1)^2$ respectively. It can therefore be represented by $S^2 - (2S-1)a_u^\dagger a_u$ in agreement with (2.6). The lowest-order matrix elements of $S_u^+ S_u^+$ and $S_u^- S_u^-$ are $\langle S | S_u^+ S_u^+ | S-2 \rangle = \langle S-2 | S_u^- S_u^- | S \rangle = [4S(2S-1)]^{1/2}$. Since $\langle S | a_u a_u | S-2 \rangle = \langle S-2 | a_u^\dagger a_u^\dagger | S \rangle = \sqrt{2}$, it follows that the proper representation for the rhombic term is

$$S_{ux}^2 - S_{uy}^2 = S(1 - 1/2S)^{1/2}(a_u a_u + a_u^\dagger a_u^\dagger), \quad (2.8)$$

which is to be compared with (2.7). Similar arguments obviously apply for the "down" sublattice operators. The anisotropic contribution to the total Hamiltonian now reads

$$\begin{aligned} \mathcal{H}_{\text{anis}} &= \sum_u \{ ES(1 - 1/2S)^{1/2}(a_u a_u + a_u^\dagger a_u^\dagger) \\ &\quad - D[S^2 - (2S-1)a_u^\dagger a_u] \} + \sum_d \{ -ES(1 - 1/2S)^{1/2} \\ &\quad \times (b_d b_d + b_d^\dagger b_d^\dagger) - D[S^2 - (2S-1)b_d^\dagger b_d] \}. \end{aligned} \quad (2.9)$$

The isotropic exchange terms in (2.1) may be expressed in terms of the boson operators by direct use of (2.2) and (2.3) when we find

$$\begin{aligned} \mathcal{H}_{\text{ex}} &= \sum_{nn'} J_1 [S^2 + 2S(a_n^\dagger a_{n'} - a_n^\dagger a_n)] \\ &\quad + \sum_{nn'}^{dd'} J_1 [S^2 + 2S(b_n^\dagger b_{n'} - b_n^\dagger b_n)] \\ &\quad + \sum_{nnn'} J_2 [-S^2 + S(a_n b_n + a_n^\dagger b_n^\dagger + a_n^\dagger a_n + b_n^\dagger b_n)]. \end{aligned} \quad (2.10)$$

The total Hamiltonian $\mathcal{H} = \mathcal{H}_{\text{anis}} + \mathcal{H}_{\text{ex}}$ is readily diagonalized by the series of canonical transformations set out in detail in Sec. 4 of Ref. 3. We find eigenvalues

$$E_{n_1 \mathbf{K} n_2 \mathbf{K}} = E_0 + S \sum_{\mathbf{K}} (n_{1\mathbf{K}} + n_{2\mathbf{K}} + 1)(a_{\mathbf{K}} b_{\mathbf{K}} - c_{\mathbf{K}}^2)^{1/2}, \quad (2.11)$$

where $n_{1\mathbf{K}}$ and $n_{2\mathbf{K}}$ are positive integers denoting the number of magnons present in each of the two degenerate spin-wave branches with wave vector \mathbf{K} , where $\sum_{\mathbf{K}}$ runs over $\frac{1}{2}N$ points in the first Brillouin zone of the reciprocal sublattice (N being the number of spins in the entire lattice), and where

$$E_0 = \frac{1}{2}ND - \frac{1}{2}NS(S+1)[J_2(0) - J_1(0) + 2D], \quad (2.12)$$

$$\begin{aligned} a_{\mathbf{K}} &= J_1(\mathbf{K}) - J_1(0) + J_2(0) \\ &\quad + 2D(1 - 1/2S) + 2E(1 - 1/2S)^{1/2}, \end{aligned} \quad (2.13a)$$

$$\begin{aligned} b_{\mathbf{K}} &= J_1(\mathbf{K}) - J_1(0) + J_2(0) \\ &\quad + 2D(1 - 1/2S) - 2E(1 - 1/2S)^{1/2}, \end{aligned} \quad (2.13b)$$

$$c_{\mathbf{K}} = J_2(\mathbf{K}). \quad (2.14)$$

¹¹ R. Kubo, Phys. Rev. **87**, 568 (1952).

Here we have written

$$\begin{aligned}
 J_1(\mathbf{K}) &= \sum_{nn} J_1 \exp[i\mathbf{K} \cdot (\mathbf{r} - \mathbf{r}_0)], \\
 J_2(\mathbf{K}) &= \sum_{nnn} J_2 \exp[i\mathbf{K} \cdot (\mathbf{r} - \mathbf{r}_0)],
 \end{aligned}
 \tag{2.15}$$

where $\sum_{nn}(\sum_{nnn})$ is a sum over all nearest neighbors (next-nearest neighbors) \mathbf{r} of \mathbf{r}_0 . We observe that the magnon energies contain the parameter E only as E^2 and its effects are therefore negligible for FeF_2 . We shall take $E=0$ in all subsequent calculations of this paper.

Putting $\mathbf{K}=0$ in Eq. (2.11) gives us an expression for the antiferromagnetic resonance frequency in the form $\omega_{\text{afmr}} = S\{[J_2(0) + 2D(1 - 1/2S)]^2 - [J_2(0)]^2\}^{1/2}$. (2.16)

For FeF_2 we require $S=2$, and the above relationship reduces to

$$\omega_{\text{afmr}} = [12Dz_2J_2 + 9D^2]^{1/2}, \tag{2.17}$$

where $z_2=8$ is the number of next-nearest neighbors of any particular ferrous ion. The antiferromagnetic resonance for FeF_2 has been observed by Ohlmann and Tinkham¹² who report a frequency $52.7 \pm 0.2 \text{ cm}^{-1}$. Equation (2.17) can now be used to give an accurate relationship between J_2 and D ; it is shown in Fig. 2. We shall include in the parameter D that small contribution to the anisotropy field which arises from dipole-dipole interactions. For FeF_2 it contributes an amount $\sim 0.3 \text{ cm}^{-1}$ to D , so that neglecting exchange anisotropy, the crystal-field contribution will be $D - 0.3 \text{ cm}^{-1}$.

Recent measurements of nuclear magnetic resonance for the fluorine anions in antiferromagnetic FeF_2 have made available the detailed temperature dependence of

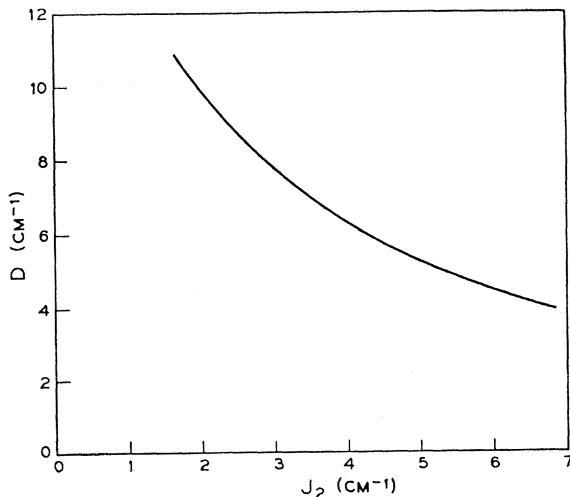


FIG. 2. The relationship between anisotropy D and exchange J_2 as determined for FeF_2 from the antiferromagnetic resonance frequency (Ref. 12) by use of Eq. (2.17).

¹² R. C. Ohlmann and M. Tinkham, Phys. Rev. **123**, 425 (1961).

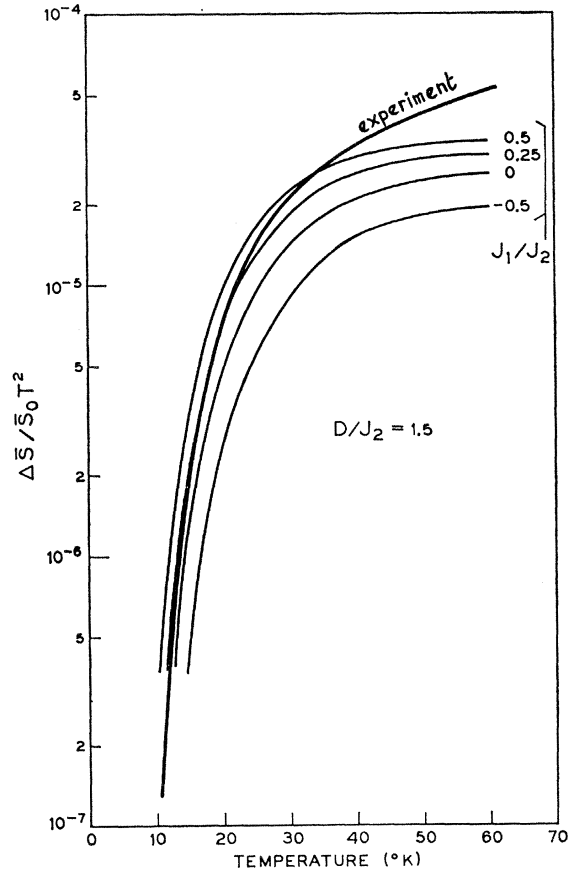


FIG. 3. Theoretical spin-wave estimates for the deviation of spin ΔS from its value S_0 at the absolute zero of temperature, plotted as a function of temperature. The curves are plotted for $D/J_2=1.5$ (the absolute magnitudes of D and J_2 being consistent with Fig. 2) and for various values of J_1/J_2 . Also shown are the experimental results from nuclear resonance experiments (Ref. 13).

sublattice magnetization in this salt.¹³ The low-temperature results are particularly significant because they should be described quite accurately by the non-interacting spin-wave theory of this section. Writing the average value of spin per site on the "up" sublattice in the form $\bar{S} = S - (2/N) \sum_u \langle a_u^\dagger a_u \rangle$ (where the pointed brackets indicate an ensemble average) and using the same canonical transformations which were used to diagonalize the Hamiltonian, we find³

$$\bar{S} = S + \frac{1}{2} - (2/N) \sum_{\mathbf{K}} \frac{a_{\mathbf{K}}}{(a_{\mathbf{K}}^2 - c_{\mathbf{K}}^2)^{1/2}} \langle n_{\mathbf{K} + \frac{1}{2}} \rangle, \tag{2.18}$$

where we have made use of the fact that $a_{\mathbf{K}} = b_{\mathbf{K}}$ for $E=0$. The ensemble average $\langle n_{\mathbf{K} + \frac{1}{2}} \rangle$ for temperature T is readily evaluated as

$$\langle n_{\mathbf{K} + \frac{1}{2}} \rangle = \frac{1}{2} \coth[S(a_{\mathbf{K}}^2 - c_{\mathbf{K}}^2)^{1/2} / 2kT], \tag{2.19}$$

giving the final spin-wave expression for sublattice spin

¹³ V. Jaccarino, in *Magnetism*, edited by G. T. Rado and H. Suhl (Academic Press Inc., New York, 1965), Vol. 2A.

in the form

$$\bar{S} = S + \frac{1}{2} - \frac{1}{2} \left\langle \frac{a_{\mathbf{K}}}{(a_{\mathbf{K}}^2 - c_{\mathbf{K}}^2)^{1/2}} \coth \left[\frac{S(a_{\mathbf{K}}^2 - c_{\mathbf{K}}^2)^{1/2}}{2kT} \right] \right\rangle_{\mathbf{K}}, \quad (2.20)$$

where $\langle \dots \rangle_{\mathbf{K}}$ is an average for \mathbf{K} running over its allowed values in the first Brillouin zone of the reciprocal sublattice.

For the FeF₂ lattice we may write

$$\begin{aligned} a_{\mathbf{K}} &= 2J_1 \cos(2K_z) - 2J_1 + 8J_2 + 3D/2, \\ c_{\mathbf{K}} &= 8J_2 \cos(K_x) \cos(K_y) \cos(K_z), \end{aligned} \quad (2.21)$$

where, in $\langle \dots \rangle_{\mathbf{K}}$, the variables K_x , K_y , K_z , run independently between $-\pi$ and π .

Using (2.20) and (2.21) we have computed the temperature dependence of sublattice magnetization for several pairs of values J_2 , D , consistent with Fig. 2, and for each pair we have plotted a set of curves for various values of J_1/J_2 . A typical set of results is shown in Fig. 3. For each value of D/J_2 it is possible to choose J_1/J_2 in such a way that the experimental spin deviation results are reproduced up to temperatures $\sim 24^\circ\text{K}$ (which is $T \sim 0.3T_N$). For higher temperatures, the theoretical spin deviations are smaller than those obtained from nuclear resonance, which is qualitatively the effect which we should expect to result from a neglect of spin-wave interactions. The combined results from antiferromagnetic resonance and from low-temperature spin deviations are therefore not sufficient to determine the problem completely. We can, however, use the latter to relate D/J_2 and J_1/J_2 and this is done in Fig. 4.

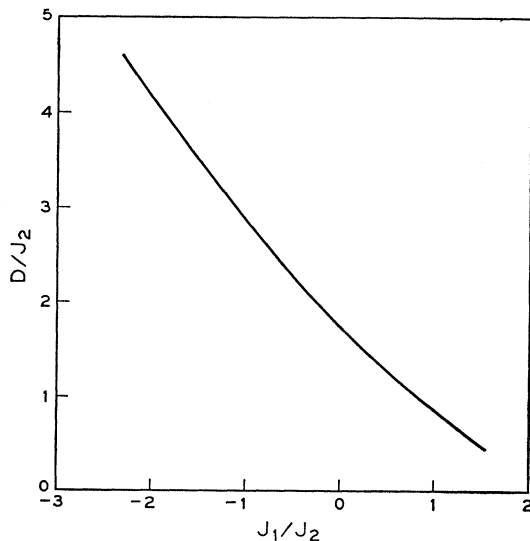


FIG. 4. The relationship between D/J_2 and J_1/J_2 , determined for FeF₂ by fitting theoretical spin-wave curves of the type shown in Fig. 3 to the measured temperature dependence of sublattice spin (Ref. 13).

Figures 2 and 4 supply us with two relationships between the three variables J_1 , J_2 , and D . In order to complete the problem we shall appeal to magnetic susceptibilities for which we now possess detailed single-crystal experimental results⁸ for temperatures up to 300°K .

3. MAGNETIC SUSCEPTIBILITIES

The magnetic susceptibility of FeF₂ has been discussed theoretically in some detail by Honma.⁵ When his work was done, however, single-crystal experimental results were not available and it was necessary to couple powder susceptibility measurements¹⁴ (which did not extend to temperatures much below T_N) with torque measurements of magnetic anisotropy.¹⁵ Also, a general lack of experimental information for low temperatures necessitated the use of a molecular-field theory for T_N as part of the procedure for estimating J_1 and J_2 . Molecular-field theories for transition temperatures are notoriously suspect and, with the extra experimental results now available, we are able to avoid transition-temperature theories for use in estimating the basic parameters of the problem.

Since the rhombic anisotropy is negligible for bulk properties, our basic Hamiltonian in the presence of an external magnetic field H may be written⁵

$$\mathcal{H} = \mathcal{H}_0 + \sum_i \mathcal{H}_{if}, \quad (3.1)$$

where

$$\mathcal{H}_0 = \sum_i -DS_{iz}^2 + \sum_{nn} J_1 \mathbf{S}_i \cdot \mathbf{S}_j + \sum_{nnn} J_2 \mathbf{S}_i \cdot \mathbf{S}_j, \quad (3.2)$$

the sums \sum_{nn} and \sum_{nnn} running, respectively, over all pairs of nearest and next-nearest neighbors i and j , and where

$$\begin{aligned} \mathcal{H}_{if} &= -\mu_B (g_{\perp} S_{ix} H_x + g_{\perp} S_{iy} H_y + g_{\parallel} S_{iz} H_z) \\ &\quad - \mu_B^2 (\Lambda_{\perp} H_x^2 + \Lambda_{\parallel} H_y^2 + \Lambda_{\parallel} H_z^2), \end{aligned} \quad (3.3)$$

where μ_B is the Bohr magneton, and g and Λ are related by

$$\begin{aligned} g_{\perp} &= 2(1 - \lambda \Lambda_{\perp}), \\ g_{\parallel} &= 2(1 - \lambda \Lambda_{\parallel}). \end{aligned} \quad (3.4)$$

The parameter λ in these equations is the spin-orbit coupling constant which will be reduced considerably from its free-ion value¹⁶ of -103 cm^{-1} . Of the parameters in \mathcal{H}_{if} , g_{\parallel} is known quite accurately from the splitting of the antiferromagnetic resonance in an external magnetic field H_z . Richards¹⁷ finds a value 2.23 ± 0.02 . Also, from an analysis of high-temperature parallel susceptibility (i.e., external field parallel to the c_0 axis), Foner⁸ finds $g_{\parallel} = 2.20 \pm 0.05$. In Foner's

¹⁴ H. Bizette and B. Tsai, *Compt. Rend.* **212**, 119 (1941).

¹⁵ J. W. Stout and L. M. Matarrese, *Rev. Mod. Phys.* **25**, 339 (1953).

¹⁶ M. Tinkham, *Proc. Roy. Soc. (London)* **A236**, 549 (1956).

¹⁷ P. L. Richards (private communication).

analysis, however, the temperature-independent terms are neglected and we shall reconsider the interpretation of susceptibility data below.

The parameter g_{\perp} is rather less accurately known. A perpendicular magnetic field does not split the antiferromagnetic resonance frequency and yields little or no information concerning g_{\perp} . Foner fits the high-temperature perpendicular susceptibility to a Curie-Weiss law to obtain $g_{\perp}=2.04\pm 0.05$; temperature-independent terms are again neglected but the fact that g_{\perp} is so close to 2 suggests that their neglect may not be serious.

We shall use molecular-field theory to analyze the Hamiltonian (3.1) both in the paramagnetic and the antiferromagnetic states. Such a theory should be adequate both for $T \gg T_N$ and for $T \ll T_N$.

The Paramagnetic State

Consider first an external field H_z parallel to the c_0 axis. The molecular-field Hamiltonian for this case is

$$\mathcal{H}_i = -DS_{iz}^2 + (z_1J_1 + z_2J_2)\bar{S}S_{iz} - g_{\perp}\mu_B H_x S_{ix} - \mu_B^2 \Lambda_z H_z^2, \quad (3.5)$$

(where $z_1=2$ and $z_2=8$) with eigenvalues

$$E_m = -Dm^2 + (z_1J_1 + z_2J_2)\bar{S}m - g_{\perp}\mu_B H_x m - \mu_B^2 \Lambda_z H_z^2, \quad (3.6)$$

where m is the azimuthal spin quantum number. The magnetic moment M_i at the site i is now given by

$$M_i = \frac{\sum_m [-(\partial E_m / \partial H_x) \exp(-E_m/kT)]}{\sum_m \exp(-E_m/kT)}. \quad (3.7)$$

In the paramagnetic state $\mu_B H_x$ and $\bar{S}(z_1J_1 + z_2J_2)$ are both very much smaller than kT and, expanding the relevant parts of the exponentials, we obtain the paramagnetic parallel susceptibility χ_{\parallel} in the form

$$\chi_{\parallel} = \frac{N g_{\perp}^2 \mu_B^2 F_{\parallel}(T)}{D + (z_1J_1 + z_2J_2)F_{\parallel}(T)} + 2N \mu_B^2 \Lambda_z, \quad (3.8)$$

where N is the total number of spins in the lattice and where

$$F_{\parallel}(T) = \frac{\sum_m Dm^2 \exp(Dm^2/kT)}{kT \sum_m \exp(Dm^2/kT)}. \quad (3.9)$$

In the temperature range of interest ($T_N < T < 300^\circ\text{K}$) evaluation of $F_{\parallel}(T)$ from (3.9) shows, to a very good approximation, that

$$D[F_{\parallel}(T)]^{-1} = \frac{1}{2}kT - 0.6D, \quad (3.10)$$

with the result that the parallel paramagnetic susceptibility may be expressed in the form

$$\chi_{\parallel} = \frac{2N g_{\perp}^2 \mu_B^2}{kT - 1.2D + 2(z_1J_1 + z_2J_2)} + 2N \mu_B^2 \Lambda_z. \quad (3.11)$$

To evaluate the perpendicular paramagnetic susceptibility, we consider a small external magnetic field in the x direction. The molecular-field Hamiltonian now reads

$$\mathcal{H}_i = -DS_{ix}^2 + (z_1J_1 + z_2J_2)\bar{S}_x S_{ix} - g_{\perp}\mu_B H_x S_{ix} - \mu_B^2 \Lambda_x H_x^2, \quad (3.12)$$

where \bar{S}_x is the average value of spin per site in the presence of the external field. Let us write this in the form

$$\mathcal{H}_i = -DS_{ix}^2 - \mu_B^2 \Lambda_x H_x^2 - \alpha S_{ix}, \quad (3.13)$$

where

$$\alpha = g_{\perp}\mu_B H_x - (z_1J_1 + z_2J_2)\bar{S}_x. \quad (3.14)$$

Treating the α term in (3.13) by second-order perturbation theory, we obtain eigenvalues E_m in this approximation as follows:

$$\begin{aligned} E_{\pm 2} &= -4D - \mu_B^2 \Lambda_x H_x^2 - \alpha^2/3D, \\ E_{\pm 1} &= -D - \mu_B^2 \Lambda_x H_x^2 - 7\alpha^2/6D, \\ E_0 &= -\mu_B^2 \Lambda_x H_x^2 + 3\alpha^2/D. \end{aligned} \quad (3.15)$$

The calculation of perpendicular susceptibility now follows in a manner analogous to that used for the parallel case. The magnetic moment M_i at the site i is given by an equation of the form (3.7) but with H_x replaced by H_x . The exponentials are expanded for small values of α and we calculate a paramagnetic perpendicular susceptibility

$$\chi_{\perp} = \frac{N g_{\perp}^2 \mu_B^2 F_{\perp}(T)}{D + (z_1J_1 + z_2J_2)F_{\perp}(T)} + 2N \mu_B^2 \Lambda_x, \quad (3.16)$$

where

$$F_{\perp}(T) = \frac{(4/3) \exp(4D/kT) + (14/3) \exp(D/kT) - 6}{2 \exp(4D/kT) + 2 \exp(D/kT) + 1}. \quad (3.17)$$

Computation of (3.17) shows, to a very good approximation, that

$$D[F_{\perp}(T)]^{-1} = \frac{1}{2}kT + 0.4D, \quad (3.18)$$

allowing us to write the perpendicular susceptibility in the form

$$\chi_{\perp} = \frac{2N g_{\perp}^2 \mu_B^2}{kT + 0.8D + 2(z_1J_1 + z_2J_2)} + 2N \mu_B^2 \Lambda_x. \quad (3.19)$$

Also of interest in passing is the fact that

$$D[F_{\parallel}(T_N)]^{-1} = z_2J_2 - z_1J_1,$$

a result which allows us to express the molecular-field parallel susceptibility at the Néel point in a rather simple form, namely,

$$\chi_{\parallel}(T_N) = \frac{N g_{\parallel}^2 \mu_B^2}{2z_2J_2} + 2N \mu_B^2 \Lambda_z, \quad (3.20)$$

which is independent of the parameter D .

The Antiferromagnetic State

As the temperature goes to zero, the susceptibility in the direction of spin alignment (χ_0) becomes equal to the temperature-independent term $2N\mu_B^2\Lambda_z$. We shall calculate the susceptibilities in the ordered state only for the case $T \rightarrow 0$. We have therefore¹⁸

$$\chi_{11}(0) = 2N\mu_B^2\Lambda_z. \quad (3.21)$$

The molecular-field Hamiltonian for the case of a perpendicular external field may be written

$$\mathfrak{H}\mathcal{C}_i = -DS_{iz}^2 - \alpha_0 S_{iz} - \alpha S_{ix} - \mu_B^2\Lambda_1 H_x^2, \quad (3.22)$$

where

$$\alpha_0 = (z_2 J_2 - z_1 J_1)\bar{S},$$

\bar{S} being the average z component of spin taking a value $\bar{S}=2$ as the temperature goes to zero (molecular-field approximation), and where α is given by (3.14). Treating the small αS_{ix} term in (3.22) by perturbation theory, we may obtain the eigenvalues E_m of $\mathfrak{H}\mathcal{C}_i$. At very low temperatures, only the lowest state with eigenvalue

$$E_2 = -4D - 2\alpha_0 - \alpha^2/(3D + \alpha_0) - \mu_B^2\Lambda_1 H_x^2 \quad (3.23)$$

is populated. Thus, the x component of magnetic moment M_{ix} on the site i is given by

$$M_{ix} = -\partial E_2 / \partial H_x = 2g_1\mu_B\alpha/(3D + \alpha_0) + 2\mu_B^2\Lambda_1 H_x. \quad (3.24)$$

Using (3.14) we find for the zero-temperature perpendicular susceptibility the result

$$\chi_{11}(0) = \frac{2Ng_1^2\mu_B^2}{3D + 4z_2J_2} + 2N\mu_B^2\Lambda_1. \quad (3.25)$$

Discussion

It is common practice in theories of antiferromagnetism to assess the anisotropy in a system by measurement of antiferromagnetic resonance and perpendicular susceptibility (in the ordered state) and use of the equation^{12,19}

$$\hbar\omega_{\text{afmr}} = g_1\mu_B(2K/\chi_{11})^{1/2}, \quad (3.26)$$

where K is the anisotropy constant of the system. Combining Eqs. (2.17) and (3.25) we obtain such a relationship if $\Lambda_1=0$, with the result that $K=3ND$. This value for anisotropy constant is in agreement with that obtained by Kanamori and Minatono²⁰ who pointed out an error in the earlier estimate of Ohlmann and Tinkham.¹² It is of interest to note that (3.26) only holds if temperature-independent contributions are

¹⁸ S. D. Silverstein and I. S. Jacobs, Phys. Rev. Letters **12**, 670 (1964).

¹⁹ J. Kanamori and M. Tachiki, J. Phys. Soc. Japan **17**, 1384 (1962).

²⁰ J. Kanamori and H. Minatono, J. Phys. Soc. Japan **17**, 1759 (1962).

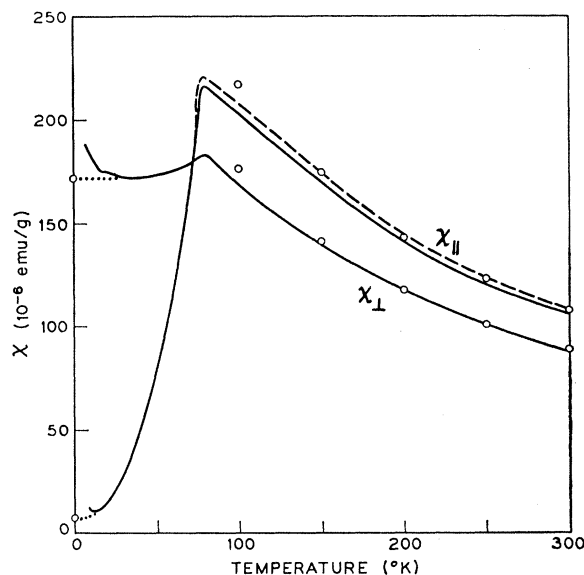


FIG. 5. Molecular-field estimates of parallel and perpendicular magnetic susceptibilities (open circles) are compared with the experimental curves given by Foner (Ref. 8). The dashed line shows the torque data of Stout and Matarrese (Ref. 15), where $\chi_{11} - \chi_{\perp}$ is plotted with respect to the experimental χ_{\perp} data. The anomalous behavior of χ as $T \rightarrow 0$ is almost certainly due to impurities and is discussed in the text.

subtracted from the experimental χ_{\perp} . Such a correction, however, is likely to be small for most cases.

We are now in a position to complete the determination of the relevant magnetic parameters for FeF₂. Firstly a few words are necessary concerning the measured susceptibility. The experimental single-crystal susceptibility measurements of Foner⁸ are shown in Fig. 5. They indicate, as expected, a nonzero value for $\chi_{11}(0)$; but the magnitude ($\sim 1.2 \times 10^{-5}$ emu/g) almost certainly includes a sizeable contribution from impurities. We say this for two reasons. Firstly, such an effect is clearly present for low-temperature measurements of χ_{\perp} and, secondly, such a large value for $\chi_{11}(0)$ is incompatible with a description of χ_{11} in the paramagnetic state unless $g_{11} \sim 2.07$. Such a value is out of the question bearing in mind the result $g_{11} = 2.23 \pm 0.02$ obtained from the splitting of the antiferromagnetic resonance lines (any possible g shift between the paramagnetic and ordered states is certainly minute compared with this discrepancy).

Low-temperature parallel susceptibility for FeF₂ has been discussed by Silverstein and Jacobs¹⁸ who find

$$\chi_{11}(0) = -N\mu_B^2 k(g_{11} - 2)/\lambda, \quad (3.27)$$

where k is an orbital reduction parameter. Using Tinkham's¹⁶ estimates for $k(\sim 0.95)$, for $\lambda(\sim 63 \text{ cm}^{-1})$, and for $g_{11}(2.25)$, which were obtained for Fe²⁺ in ZnF₂, they find $\chi_{11}(0) \sim 1.0 \times 10^{-5}$ emu/g. More recent work²¹ favors a value $k \sim 0.85 \pm 0.05$ for transition-

²¹ J. Owen and J. H. M. Thornley, Rept. Progr. Phys. **29**, 675 (1966).

metal ions and, anticipating our final result $g_{11}=2.21$, we tend to favor a value $\chi_{11}(0)\sim 0.7\times 10^{-5}$ emu/g for FeF_2 .

Our task now reduces to the following. We have seven variables, J_1 , J_2 , D , g_{11} , g_{\perp} , Λ_{11} , and Λ_{\perp} , with six of them independent [since $(g_{11}-2)/(g_{\perp}-2)=\Lambda_{11}/\Lambda_{\perp}$ from Eq. (3.4)]. We hope to be able to choose them in such a way that we can explain nine separate experimental results which are: antiferromagnetic resonance, its splitting in an external magnetic field H_z , sublattice magnetization as a function of temperature in the spin-wave region, $\chi_{11}(0)$, $\chi_{\perp}(0)$, $\chi_{11}(T\gg T_N)$ and its temperature derivative, $\chi_{\perp}(T\gg T_N)$ and its temperature derivative. The problem is therefore comfortably overdetermined and we can avoid having to make use of results for which the available theory is suspect, e.g., $\chi_{11}(T_N)$, $\chi_{\perp}(T_N)$, and T_N itself.

The best agreement between theory and experiment for the above properties is obtained for $g_{11}=2.21$, when we can account for all of them within experimental error [allowing for the above-mentioned reservations concerning the experimental value of $\chi_{11}(0)$] by putting

$$\begin{aligned} D &= 6.5 \pm 0.3 \text{ cm}^{-1}, \\ J_2 &= 3.85 \pm 0.2 \text{ cm}^{-1}, \\ J_1/J_2 &= 0.1 \pm 0.25, \\ g_{\perp} &= 2.08 \pm 0.04, \end{aligned} \quad (3.28)$$

$$\Lambda_z \sim 0.0015 \text{ cm}, \quad \Lambda_{\perp} \sim 0.0005 \text{ cm}.$$

These values are consistent with Figs. 2 and 4 for antiferromagnetic resonance and sublattice magnetization, and the theoretical estimates for susceptibility (as obtained by use of the molecular-field results of the present section) are compared with experiment in Fig. 5. Also shown in Fig. 5 is the torque data for $\chi_{\perp}-\chi_{11}$ as obtained by Stout and Mataresse¹⁵ which (following Foner⁸) we plot with respect to the experimental χ_{\perp} data.

The value for the anisotropy parameter D is in good agreement with that obtained earlier by Kanamori and Minatono.²⁰ The crystal-field contribution to D is $6.2 \pm 0.3 \text{ cm}^{-1}$ and is to be compared with the value $7.3 \pm 0.7 \text{ cm}^{-1}$ found by Tinkham⁴ for Fe^{2+} in ZnF_2 . It seems clear that the exchange J_1 is small compared with J_2 (a situation which has also been found to exist in MnF_2 and CoF_2) but the question of its sign must remain open.

4. THE NÉEL TEMPERATURE

From (3.28) we find a value $D/J_2=1.7 \pm 0.2$ which indicates that FeF_2 is a salt for which the effects of anisotropy are quite large; certainly outside the "small anisotropy" range for which the Green's-function theory of Paper I was primarily developed. Nevertheless, as far as transition temperature is concerned, FeF_2 provides a good test case for the available theories, because the anisotropy is sufficiently large to provide a

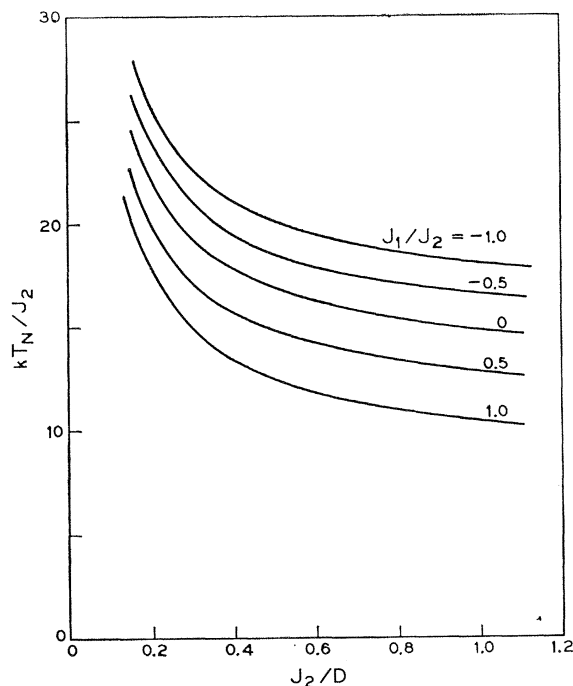


FIG. 6. Néel temperature, as calculated from the Green's-function theory developed in Paper I, is plotted as a function of J_2/D for several values of J_1/J_2 .

shift of Néel temperature (from the equivalent isotropic case) which is much greater than the likely error in theoretical estimates for the isotropic case. This means that we are able to compare the theories not only for their absolute estimates of T_N , but also for the predicted sensitivity of transition temperature to crystal-field anisotropy.

The theory of Paper I is readily adapted for use in the present case. In the absence of an external field, the Hamiltonian to be used for the magnetic properties of FeF_2 is that given in Eq. (3.2). The Néel temperature, in the Green's-function approximation of Paper I, follows from Eqs. (5.9) and (5.10) of Paper I, where

$$\lambda = 8J_2 \cos K_x \cos K_y \cos K_z, \quad (4.1)$$

$$\mu = 2J_1 \cos 2K_z - 2J_1 + 8J_2 + 2D\Gamma(T_N), \quad (4.2)$$

where $\Gamma(T_N)$ for the case $S=2$ is equal to $21/40$. All anisotropy has been included as a crystal-field term; the error involved in treating the small dipolar contribution in this way is completely insignificant in the present context. The resulting transition temperature has been computed as a function of J_2/D for various values of J_1/J_2 and the details are shown in Fig. 6.

We find that the theoretical transition temperature is very insensitive to the uncertainty in J_1/J_2 [which is expressed in Eq. (3.28)] provided that the variables J_1 , J_2 , and D , are chosen to be consistent with the very accurate antiferromagnetic resonance and the sublattice magnetization conditions of Figs. 2 and 4. The

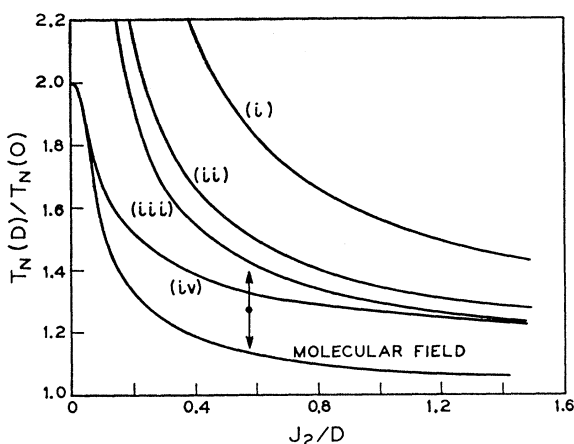


FIG. 7. The ratio $T_N(D)/T_N(0)$, where $T_N(D)$ is the Néel temperature in the presence of crystal-field anisotropy D , is plotted as a function of J_2/D for highly anisotropic systems. Curves (i), (ii), and (iii) are calculated from random-phase Green's-function theories, where the anisotropy terms are decoupled, respectively, according to Narath (Ref. 10), Anderson and Callen (Ref. 9), and the theory of Paper I. Curve (iv) is an interpolation between molecular-field theory, for extremes of high anisotropy, and curve (iii), for intermediate to small values of anisotropy. The various curves are to be compared with the experimental data for FeF_2 which are shown for $J_2/D \approx 0.57$.

Néel temperature is therefore determined very dominantly by the spin-wave energy gap and the dependence of the long-wavelength magnon energies upon wave vector. This not very surprising result allows us to determine the theoretical Néel temperature quite precisely, not only for the theory of Paper I, but also for the Anderson-Callen⁹ and the Narath¹⁰ approximations, and for molecular-field theory. The numerical results are displayed in Table I and are to be compared with the experimentally observed Néel point which, for FeF_2 , is^{8,22} $T_N \sim 79^\circ\text{K}$. We find that all the theories predict a Néel temperature which is too high, but that the theory of Paper I has the least error. Moreover, we recall from Paper I that all the Green's-function estimates break down in the limit of large anisotropy and are expected to show anomalously high transition temperatures for highly anisotropic systems. This effect can be studied in a little more detail as follows.

In Fig. 7 we show the estimates of the various theories in question for $T_N(D)/T_N(0)$ as a function of J_2/D in the large anisotropy range, where $T_N(D)$ is the Néel temperature for a system with an axial crystal-field parameter D . These curves are calculated for a body-centered tetragonal lattice with nearest-neighbor exchange $J_1=0$, and for spin quantum number $S=2$. They are directly applicable for FeF_2 if we put $z_2 J_2$

$= 43.5^\circ\text{K}$ and $D/J_2=1.74$. We note that all the Green's-function approximations show $T_N(D)$ to diverge as $J_2/D \rightarrow 0$. The molecular-field theory, on the other hand, gives a value $T_N(D)/T_N(0) \rightarrow 2$ in this same extreme anisotropy (Ising) limit. Using Eq. (6.4) from Paper I, we expect the true limiting value to be within a few percent of 2.14. Thus, for this feature at least, the molecular-field theory is good.

To compare the various theories with experiment for $T_N(D)/T_N(0)$ it is necessary to have a fairly reliable value for the Néel temperature of an isotropic Heisenberg antiferromagnet. We have used the estimate obtained from the random-phase Green's-function approximation. For $S=2$, this theory gives a Curie temperature for the isotropic Heisenberg ferromagnet which is only some 3% removed from the generally accepted "best available" results of Rushbrooke and Wood.²³ Although rather less work has been done on antiferromagnetic transition temperatures, indications are that the latter cannot be very far removed from their equivalent ferromagnetic transition temperatures; indeed, the theories discussed in the present paper all predict the equality of the two temperatures. Thus, the $S=2$ random-phase Green's-function result for $T_N(0)$ is not likely to be in error by more than ten percent, in which case we find (for $J_1=0$) $T_N(0)=11.5J_2$ and, by substituting that value of J_2 applicable for FeF_2 , it follows that $T_N(0)=62.4^\circ\text{K} \pm \sim 10\%$.

Coupling this result with the measured Néel temperature $T_N(D)=79^\circ\text{K}$ for FeF_2 , we find a value $T_N(D)/T_N(0)=1.27 \pm 0.12$ for anisotropy $D/J_2=1.74$, and this range of values is shown in Fig. 7. It is clear that the molecular-field theory underestimates the sensitivity of transition temperature to crystal-field anisotropy whereas the Green's-function approximations all overestimate it. Since molecular-field theory badly overestimates transition temperatures for the isotropic case, its accuracy improves as anisotropy increases. The theory of Paper I is seen to be the most satisfactory of the Green's-function approaches and in Fig. 7 we have also drawn a curve which interpolates between the results of the Paper I theory for intermediate values of anisotropy and the molecular-field theory for highly anisotropic systems. This curve probably represents fairly accurately the variation of transition temperature with anisotropy for real systems. For example, it predicts a Néel temperature of 83°K for FeF_2 which is to be compared with the experimental 79°K . It would also indicate that the "small anisotropy" approximation of Paper I is probably quite good for values of $D \lesssim J_2$.

²² J. W. Stout and E. Catalano, J. Chem. Phys. 23, 1803 (1955).

²³ G. S. Rushbrooke and P. J. Wood, Mol. Phys. 1, 257 (1958).